Eighth International Conference on
STEEL AND ALUMINIUM STRUCTURES
Edited by B. Young & Y. Cai
Hong Kong, China, December 7 – 9, 2016

# NUMERICAL STUDY OF SIMPLE AND RIGID BEAM-COLUMN JOINTS SUBJECT TO IMPACT LOAD

**K. CHEN[a], K. H. TAN[a] and B. YANG[b,c]**

[a] School of Civil and Environmental Engineering, Nanyang Technological University, Singapore
E-mails: kchen006@e.ntu.edu.sg, ckhtan@ntu.edu.sg

[b] Key Laboratory of New Technology for Construction of Cities in Mountain Area (Chongqing University), Ministry of Education, Chongqing 400045, China
E-mail: yang0206@cqu.edu.cn

[c] School of Civil Engineering, Chongqing University, Chongqing, China

**Keywords:** Beam-column joint; Fin plate; WUF-B; Impact load; Middle column removal scenario.

**Abstract.** *Beam-column joints are of great importance to the integrity of steel structures. In the literature, experimental research on several types of steel beam-column joints, such as end plate and web cleat joints under dynamic loads have been conducted. However, for commonly-used simple and rigid joints including fin plate (or shear tab) and welded unreinforced flanges bolted web (WUF-B) joints, numerical and experimental research studies are still rare. In this paper, an experimental test program of two steel joint specimens is presented. Numerical simulations on these two types of joints are conducted using commercial software LS-DYNA. The finite element modeling techniques are introduced and validated against both test data from the literature and a trial test on simply-supported beam conducted by the authors. Numerical predictions of two beam-column joint specimens are presented and the behavior of both fin plate and WUF-B joints is revealed and discussed. Using validated numerical models, governing parameters such as hammer mass and velocity are studied.*

## 1 INTRODUCTION

Beam-column joints play an important role in load-bearing capacity of steel frame structures. The contribution of beam-column joints to global structural resistance is of great importance when steel structures are subject to extreme loads such as impact, or explosion, which may lead to progressive collapse of the whole structure.

For the past few decades, especially after the disastrous terrorist attack on the World Trade Center on September 11th 2001, several technical design documents have been released, among which DOD [1]and GSA [2] guidelines are most commonly used. In these documents, design criteria on the integrity of steel beam-column joints are provided based on previous research efforts on seismic design. However, it was pointed out that these criteria may not be suitable at all for structures subject to progressive collapse scenarios [3, 4] through pseudo-static empirical studies.

Other than pseudo-static studies, researchers tend to study more realistic dynamic scenarios for beam-column joints. Liu et al. [5-7] conducted free-fall tests on both flush end-plate and bolted angle joints subject to middle column removal scenario along with numerical simulations. Dynamic increase factors provided by design guidelines were reviewed based on these studies. Tyas et al.[8] and Rahbari et al.[9] developed a comprehensive test rig to study the behavior of web cleat joints loaded by pneumatically activated loading rams. Failure modes and different governing parameters (such as thickness of web cleats) were investigated. Karns et al. [10] conducted real air blast tests on traditional (WUF-B) and Sideplate® moment connections. It was found that middle column removal scenario served as a credible replica of blast-induced initial damage. However, blast test scenarios are very costly and thus, it is difficult for other researchers to repeat the experiments themselves. More recently, Grimsmo el al.[11, 12] conducted experimental and numerical studies on extended end plate joints subject to impact load from high speed trolley. Different failure modes were observed for gravity load direction and reversed load direction. Up to now, very few studies focused on fin plate and WUF-B joints subject to dynamic loads. Fin plate joints are typical of simple pinned joints in steel frames which are designed to withstand gravity load. On the other hand, WUF-B joints are semi-rigid or rigid joints depending on the depth of the beam section.

In this study, impact load under middle column removal scenario was chosen as a cost-effective simplification of progressive collapse scenario based on DOD [1]. The impact load was applied by an MTS drop-weight test machine in the Protective Engineering laboratory of Nanyang Technological University (NTU). A test program consisting of two beam-column joints was introduced and numerical studies were conducted based on validation against a simply-supported beam test and previous test data in the literature.

## 2 INTRODUCTION OF EXPERIMENTAL TEST PROGRAM

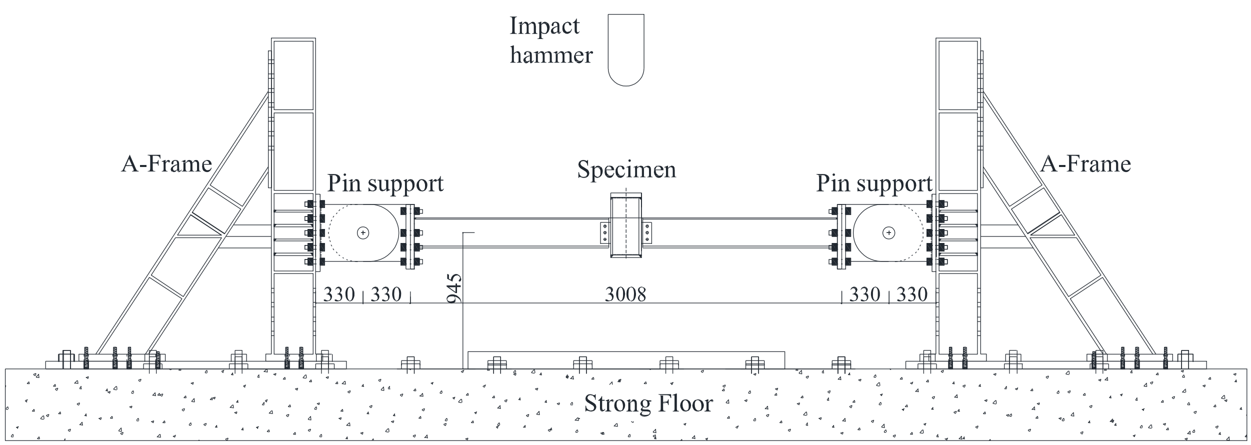


Figure 1 Front view of test set-up

An MTS drop-weight test machine was used to apply impact load in the test program. The basic drop-weight of the hammer is 510kg including a load cell system. The drop-weight can be increased to 810kg by adding 10 pieces of steel plates each weighing 30kg. The free movement height of the hammer can be up to 4m. However, when considering the height of test specimens, the dropping height is limited to 3m.

Figure 1 shows the front view of the test set-up. The impact hammer is centered to the axis of the middle column stub. Two pinned supports are used to simulate the inflection points located at the middle span of beams subject to point load at the middle column stub. Therefore, the beam span of the prototype structure is 3668 mm, smaller than a typical full-scale steel frame to accommodate the limited space in the laboratory. In this test program, two specimens were designed according to Eurocode 3 [13] and AISC 360-10 [14] as shown in Figure 2. Specimen FP was a simple joint with fin plate connection and specimen WUF-B was a rigid joint with welded unreinforced top-and-bottom flanges and bolted web connection. These two types of joints were selected because of their common applications in steel frames. By keeping the same beam section and the web connection, the contribution of welded beam flanges can be investigated through comparing the behavior of these two specimens. Grade S355 steel was used for universal beams, columns and other steel plates. For fin plates, mild steel Grade S275 was used to obtain a ductile failure mode. To avoid any brittle failure of bolts, Grade 10.9 M20 bolts were used for the web connection.

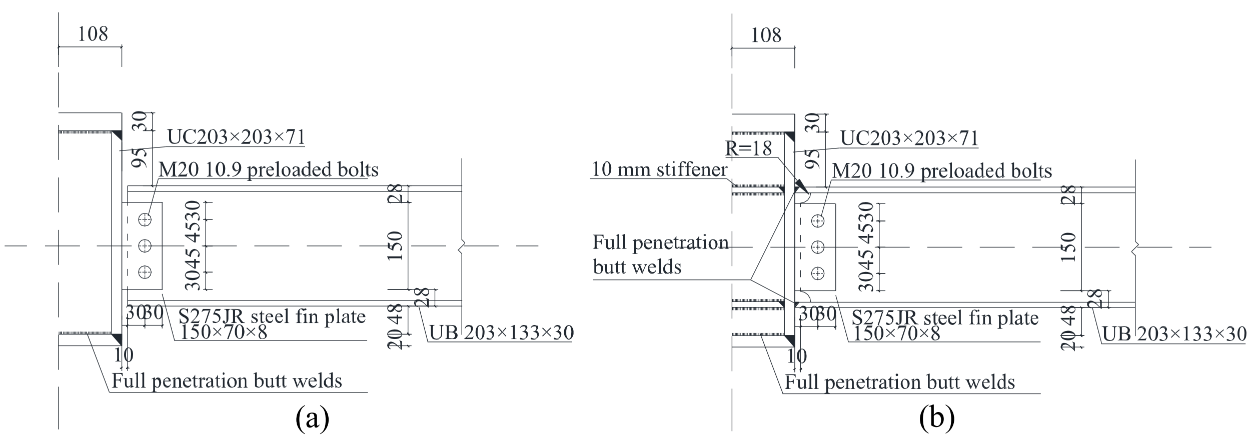


Figure 2 Detailing of connection for joint specimens: (a) Fin plate; (b) WUF-B

Before conducting the actual tests, numerical simulations were conducted to predict the behavior of these two specimens. Modeling techniques and validation will be introduced in the following section.

## 3 MODELING TECHNIQUES AND VALIDATION

The commercial software LS-DYNA [15] was chosen to build finite element (FE) models due to its common usage in dynamic explicit analyses. True stress-strain constitutive curves for each material should be transformed from engineering stress-strain curves, which were directly obtained from material tests. It is noteworthy that this transformation can only be applied before necking occurs since after this point, the assumption of uniform deformation along steel coupons will be invalid. After necking, a linear increasing curve with a failure point was used. Since the value of failure strain is highly dependent on mesh size, slight adjustment for each individual model was made. However, typical values of failure strain for high strength bolts and uniform I-shape steel cross sections were 0.1 and 0.5, respectively.

Plastic kinematic model with isotropic hardening was used in FE simulations. This material model adopted Cowper-Symonds model to consider strain-rate effect of steel material, which scales the yield strength by the strain-rate dependent factor as shown below:

$$\sigma_Y = [1 + (\frac{\varepsilon}{C})^{\frac{1}{p}}](\sigma_0 + \beta E_p \varepsilon_p^{eff}) \tag{1}$$

where $\sigma_0$ is the initial yield strength, $\varepsilon$ is the strain rate, $C$ and $P$ are the Cowper-Symonds strain-rate parameters, $\varepsilon_p^{eff}$ is the effective plastic strain, and $E_{\tan}$ is the plastic hardening modulus which is given by

$$E_p = \frac{E_{\tan} E}{E - E_{\tan}} \tag{2}$$

Solid element S164, an 8-node brick element was used for most of the three dimensional model. It uses reduced (one point) integration plus viscous hourglass control for faster element formulation. For thin-walled parts such as I-shape columns and beams, fin plates and other steel plates, at least two layers of solid elements were used in the thickness direction. More layers were required at locations with expected large deformation, such as the fin plate. In other directions, the mesh size was generally kept the same to form cuboid elements. At locations with small deformation, a larger mesh was used to save CPU time. At locations of bolt holes, at least 32 divisions were used to form a smooth circle. Hammer and pin were quite rigid with negligible deformation so that they were meshed with tetrahedrons with various sizes at different locations. The typical edge length ranged from 20 to 150 mm. At locations where there were contact surfaces such as hammer head and bracket holes, the mesh size was refined to be as small as 2mm.Though high strength bolts were used to avoid any bolt failures, they were meshed with a fine size ranging from around 2 to 5mm, to capture deformations of bolt shanks. All cambered contact surfaces used a refined mesh in comparison with adjacent parts.

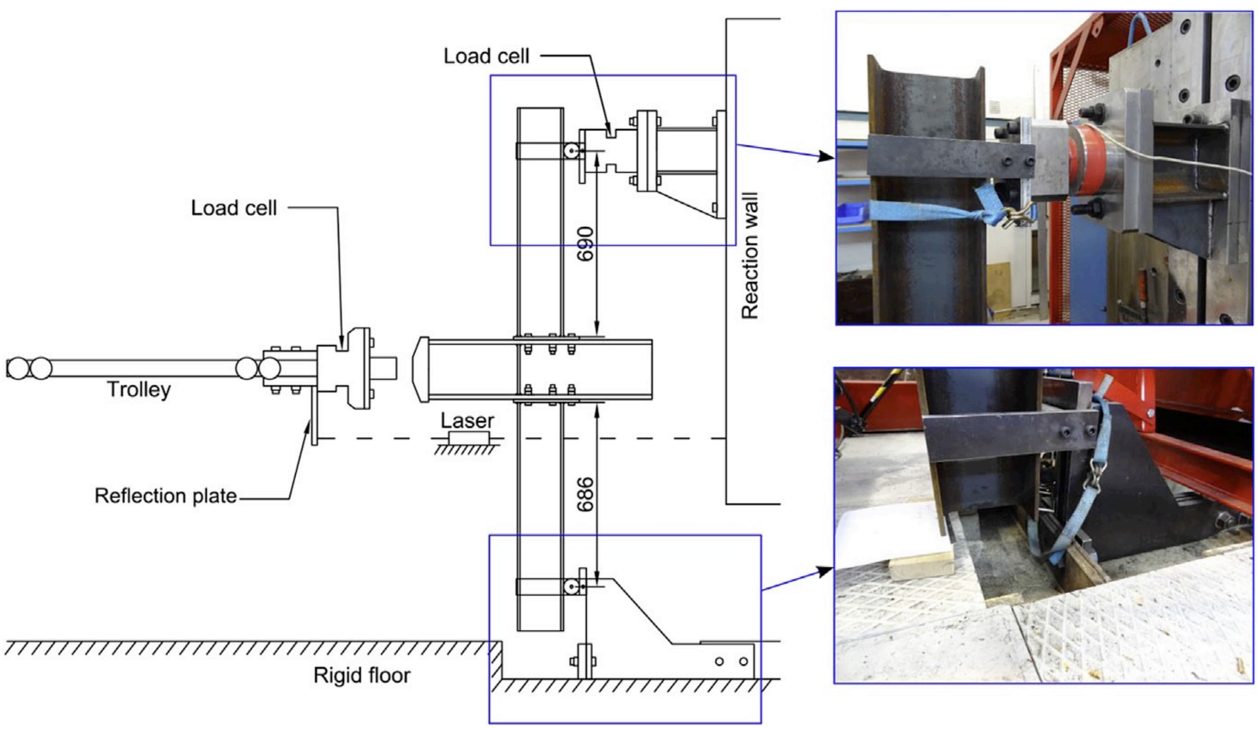


Figure 3 Test set-up in the dynamic tests by Grismsmo et al.

Surface-to-surface contact (automatic contact options) was established when a surface of one body penetrates through the surface of another body. Surface-to-surface contact is the most general type of contact as it is commonly used for bodies that have arbitrary shapes and with relatively large contact areas. In this study, contact surface pairs were established as follows: 1) bolt shanks and fin plates or beam web; 2) bolt heads or nuts and fin plates or beam web; 3) fin plates and beam web; 4) beam top flange and steel profile decking; 5) pin and bracket holes; 6) hammer head and column stub. A friction coefficient of 0.3 was used. Welds were simulated as surface-to-surface contact with tie option. This assumption gave reasonable results if there was no failure of welds.

To validate the modeling technique, test specimens conducted by Grismsmo et al. [11] were simulated by LS-DYNA. In their test program, eight beam-column joints with end plate connection were impacted by a 727 kg horizontal trolley with different velocities. The test set-up is shown in Figure 3. Specimens LS-RLD-5 and LS-DLD-6 were modeled because they were impacted by similar velocities, which were 6 m/s and 7.89 m/s, respectively. Figure 4 shows a comparison between finite element predictions and experimental results on impact force versus column displacement of these two specimens. It can be seen that the amplitude of contact force was replicated by FE models well. Apart from the subsequent colliding displacement, the first few impulses of simulations agreed well with test results.

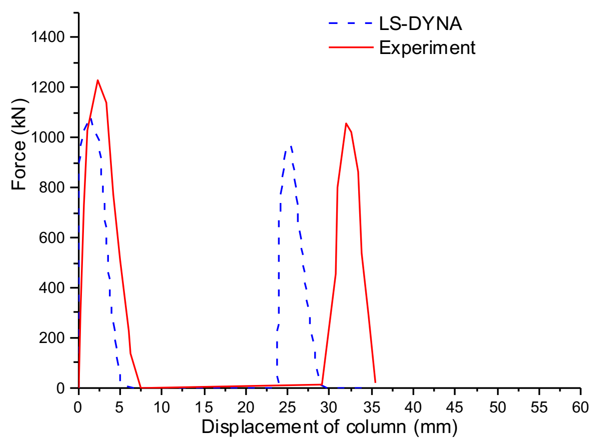


(a)

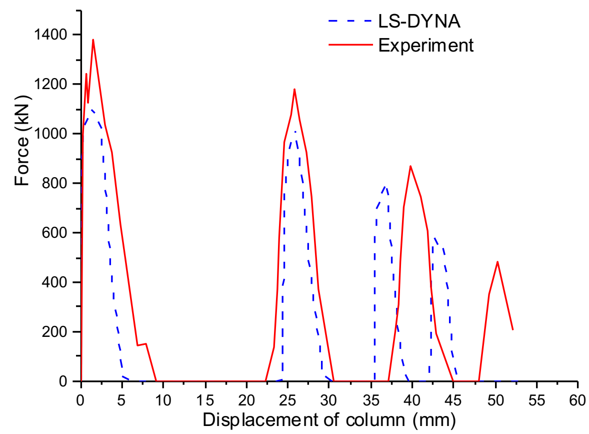


(b)

Figure 4 Comparison between impact force versus middle column displacement curves from experimental test and numerical analyses: (a) Specimen LS-RLD-5; (b) Specimen LS-DLD-6

To further validate the amplitude of the impact force, a trial test on a simply-supported beam was conducted in Protective engineering laboratory at NTU. The test set-up is shown in Figure 5(a). Grade S275 UB 254×102×25 beam with a center-to-center span of 1400 mm was tested under impact load from a 510 kg hammer with a round head. The dropping height of the hammer was 100 mm and its estimated velocity was 1.438 m/s. The impact force generated by the collision of the hammer head with the specimen was obtained by a Kristler type 9393 load cell with 1000 kN capacity as shown in Figure 5(a). Figure 5(b) shows a full-scale specimen modeled by LS-DYNA. An initial velocity of 1.438 m/s, which was the same as the trial test, was applied to the hammer.

A comparison between the impact forces captured by the load cell in the test and LS-DYNA simulation is shown in Figure 6. It can be seen that the impact force obtained from the FE simulation agreed well with that measured by the load cell in the trial test. It is worthy to note that sine waves were observed by both FE simulation and experiment test. The possible cause is the free vibration of the simply-supported beam. This validation mainly focuses on the major shape of impact force and its duration. More investigation is needed if the modal vibration of the test specimen is the major research objective.

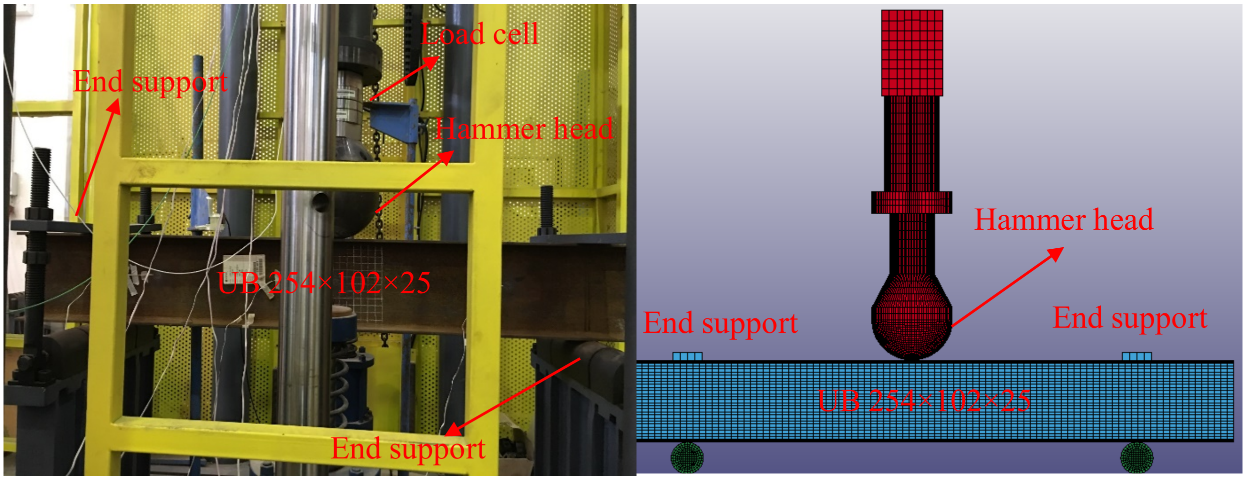


(a) (b)

Figure 5 Test set-up of simply-supported beam: (a) Physical test; (b) Numerical simulation.

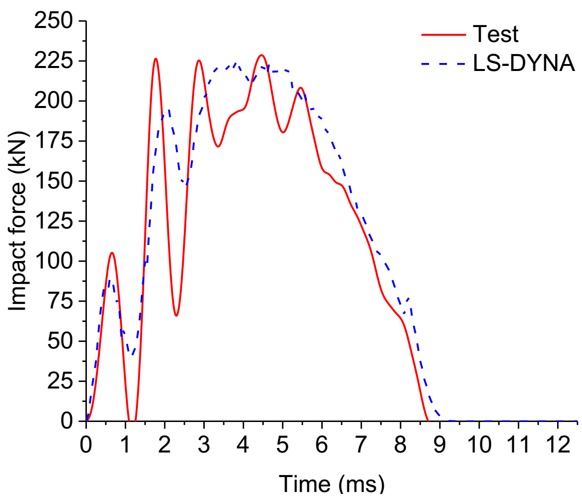


Figure 6 Force versus time curves

# 4 PARAMETRIC STUDY

After validating the modeling techniques, a parametric study on test specimens was conducted using LS-DYNA models as shown in Figure 7. Due to symmetry, only one-half of each specimen was modeled. Major parameters investigated are listed in Table 1, including connection type, hammer mass, impact velocity and momentum.

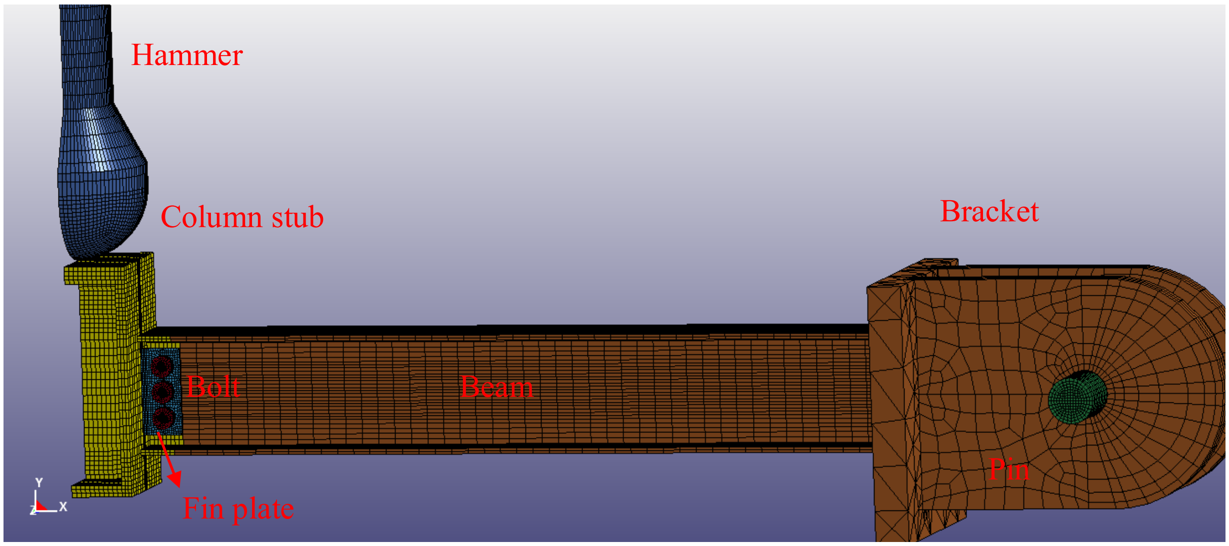


Figure 7 FE model in LS-DYNA

In the numerical analyses, the elastic modulus of all steel materials was defined as 200GPa. For S275 and S355 steels, typical values of yield strength were defined as 323 MPa and 385 MPa, respectively. Tangent modulus was defined as 763 MPa. For Grade 10.9 bolts, yield strength was defined as 900 MPa. Although the true strength of bolts was greater, using the nominal value did not give any failure of bolt shanks. In this study, the strain-rate effect was considered by using coefficients *C* and *P* of Cowper-Symonds model as 6844 and 3.91, respectively, which were based on Abramowicz and Jones [16]. Figure 8 shows the mesh size adopted in the numerical models. It should be noted that they were not drawn with the same scaling factor.

Table 1 Summary of numerical test models

| ID | Connection | Hammer (kg) | Height (m) | Velocity (m/s) | Energy (J) | Momentum (kgm/s) |
|---|---|---|---|---|---|---|
| FP-M510H3 | Fin plate | 510 | 3 | 7.668 | 14994 | 3911 |
| FP-M510H1.2 | Fin plate | 510 | 1.2 | 4.850 | 5998 | 2473 |
| FP-M810H1.2 | Fin plate | 810 | 1.2 | 4.850 | 9526 | 3929 |
| W-M810H3 | WUF-B | 810 | 3 | 7.668 | 23814 | 6211 |
| W-M810H1.2 | WUF-B | 810 | 1.2 | 4.850 | 9526 | 3929 |
| W-M510H3 | WUF-B | 510 | 3 | 7.668 | 14994 | 3911 |

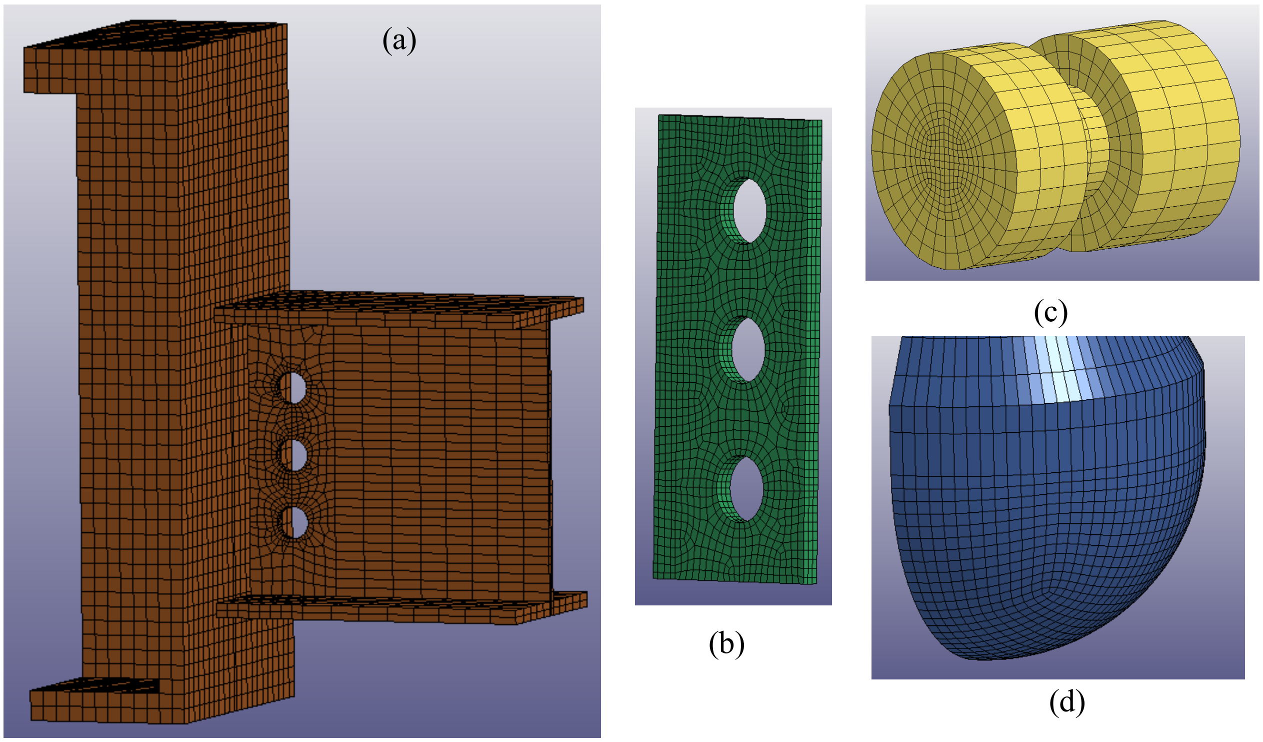

Figure 8 Mesh sizes for different part of specimens: (a) Beam and column stubs; (b) Fin plate; (c) Bolts; (d) Hammer head.

## 5 RESULTS AND DISCUSSIONS

Impact force versus middle column displacement curves obtained from numerical parametric analyses are shown in Figures 9 to 12.

Figure 9 shows the impact force versus middle column displacement curves of specimens subject to impact loads from the same mass but different velocities. Curves of fin plate and WUF-B specimens are shown in Figures 9(a) and (b), respectively. It can be seen that greater velocity generated greater impact force and larger deformation for both types of joint specimens. This was because the hammer with a greater velocity had larger impact energy. It should be noted that the impact force did not increase linearly with the impact energy because 2.50 times larger impact energy generated only 1.41 and 1.35 times greater forces for fin plate and WUF-B specimens, respectively. This phenomenon may be attributed to the quantity of exchanged and consumed impact energy, which requires further study and is not in the scope of this paper.

When keeping the same velocity while increasing the mass, the corresponding change in the impact force was negligible even though the displacement increased slightly, as shown in Figure 10. It means 1.59 times larger impact energy did not cause much difference (1.01 times greater) in the impact forces for both fin plate and WUF-B specimens. By comparing the results from Figures 9 and 10, it was found that for both types of joint specimens, the velocity of impact hammer had a greater effect on impact force compared to the dropping-weight.

From Figure 11 by keeping the same momentum of the hammer, a greater velocity with smaller mass led to a greater impact force for both types of joint specimens. For WUF-B specimen, it also led to a much larger displacement as shown in Figure 9(b). This was because the impact energy of greater velocity was larger by comparing specimens W-M510H3 and W-M810H1.2 in Table 1. For fin plate specimen, the final displacements under both impact loads were similar because the loads were larger than the resistance of this type of simple joint. Under both impact loading conditions, the fin plate specimen was totally damaged so that the middle column stub moved freely to a displacement of more than 250 mm until the end of analyses. By contrast, the middle column stub of specimen W-M810H1.2 rebounded back to 48 mm, which was caused by the resilience of its elastic deformation.

A comparison between responses of fin plate and WUF-B joint specimens subject to different impact loads is shown in Figure 12. WUF-B joint specimen had greater impact force when subject to the same impact load. The peak values were 807 kN and 869 kN for impact loads of 810 kg at 4.850 m/s and 510 kg at 7.668 m/s, respectively. The values for fin plate joint specimen were 524 kN and 660 kN, which were much smaller. This was because the WUF-B joint specimen was much stiffer. Its peak displacement was about one-quarter of the fin plate joint specimen. It can be concluded that the WUF-B joint had much greater resistance against the impact load. The contribution of welded top and bottom beam flanges was shown to be adequate to resist the maximum load of the impact machine, which was 810 kg at 7.668 m/s. Without welding the top and bottom beam flanges, the fin plate joint specimen was totally damaged by a small impact load, which was 510 kg at 4.850 m/s, as shown in Figure 9(a).

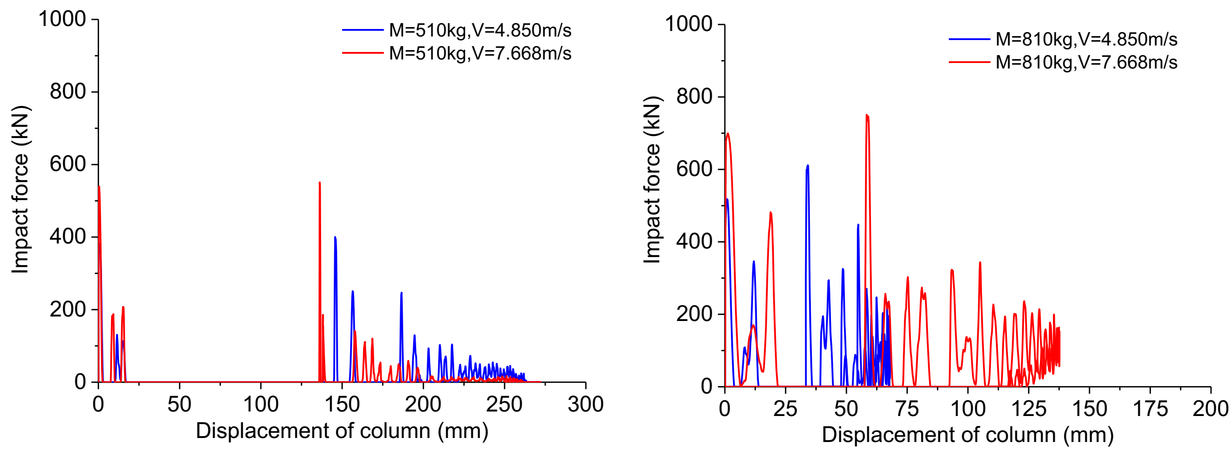


(a) (b)

Figure 9 Comparison between impact force versus middle column displacement curves obtained from different hammer velocities: (a) Fin plate specimen; (b) WUF-B specimen.

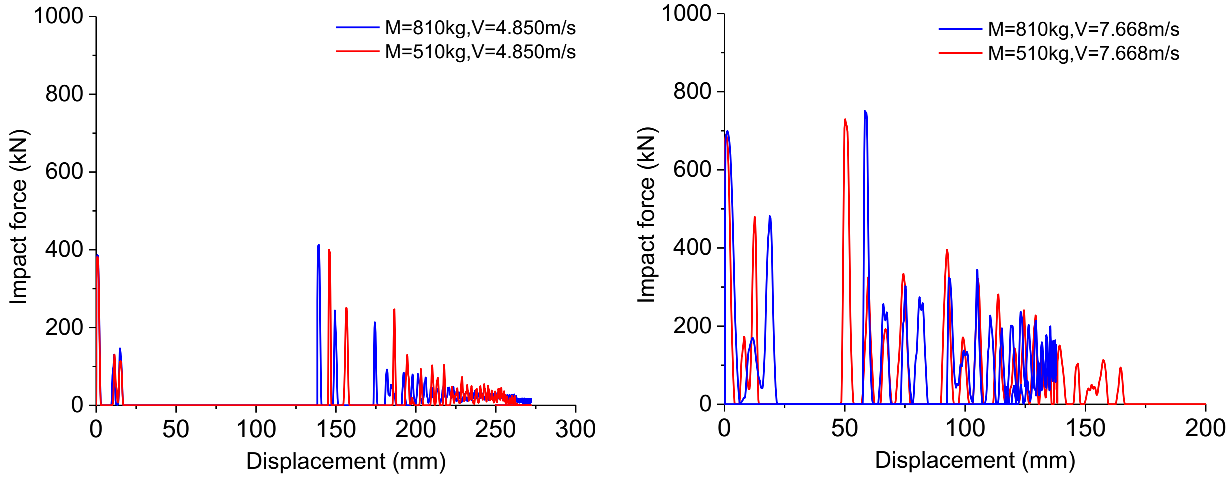


(a) (b)

Figure 10 Comparison between impact force versus middle column displacement curves obtained from different hammer mass: (a) Fin plate specimen; (b) WUF-B specimen.

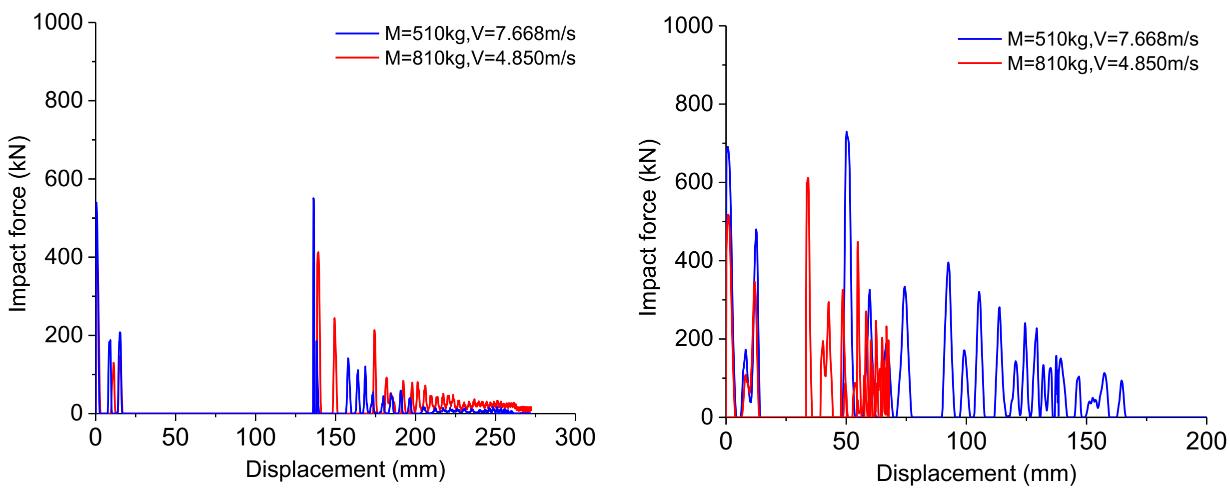


(a) (b)

Figure 11 Comparison between impact force versus middle column displacement curves obtained from same momentum: (a) Fin plate specimen; (b) WUF-B specimen.

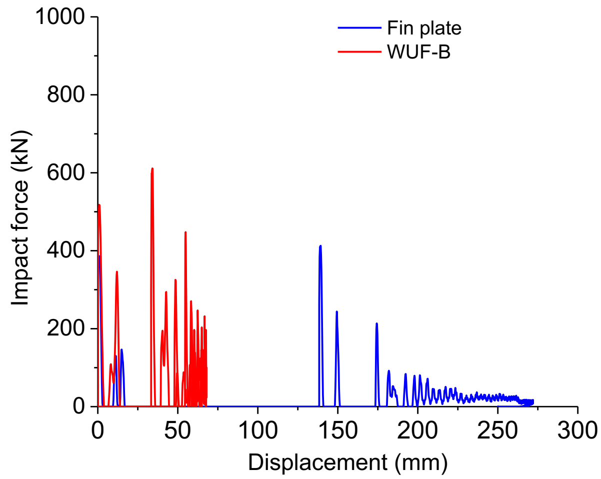


(a)

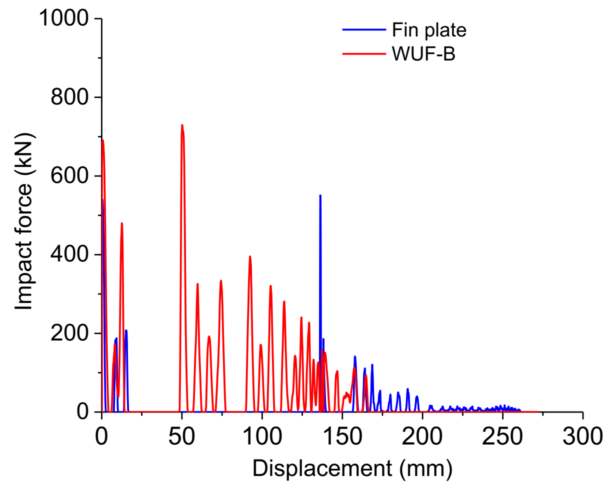


(b)

Figure 12 Comparison between impact force versus middle column displacement curves obtained from different types of joints: (a) M=810kg V=4.850m/s; (b) M=510kg V=7.668m/s.

## 6 CONCLUSIONS

In this study, a test program on two types of beam-column joints (viz. fin plate joint and WUF-B joint) subject to impact load, was presented. Numerical simulations on these specimens were conducted. The numerical analyses were validated against both previous test results from the literature and a drop-weight test conducted in NTU. A parametric study was conducted for four parameters, i.e. velocity, mass, momentum of the impact hammer and the connection type. Based on the parametric study, conclusions are drawn as follows:

- The velocity of impact hammer has a greater effect on impact force compared to the dropping-weight;
- The contribution of welded top and bottom beam flanges to the integrity of beam-column joint is adequate to resist the maximum load of the impact machine, so that the resistance of the WUF-B joint is much greater than the fin plate joint;
- Greater impact force will be generated in the stiffer joint when subject to the same impact load.

## REFERENCES


[1] *Design of buildings to resist progressive collapse.* UFC 4-023-03, Washington, D.C., U.S., Department of Defense, 2013.

[2] *Alternate path analysis and design guidelines for progressive collapse resistance.* GSA 2013, Washington, D.C., U.S., General Serviced Administration, 2013.

[3] Yang B., Tan K.H., "Experimental tests of different types of bolted steel beam–column joints under a central-column-removal scenario", *Engineering Structures*, 54, 112-130, 2013a.

[4] Yang B., Tan K.H., "Robustness of bolted-angle connections against progressive collapse: Mechanical modelling of bolted-angle connections under tension", *Engineering Structures*, 57, 153-168, 2013b.

[5] Liu C., Fung T.C., Tan K.H., "Dynamic performance of flush end-plate beam-column connections and design applications in progressive collapse", *Journal of Structural Engineering*, 142, 04015074, 2015b.

[6] Liu C., Tan K.H., Fung T.C., "Dynamic behaviour of web cleat connections subjected to sudden column removal scenario", *Journal of Constructional Steel Research*, 86, 92-106, 2013.

[7] Liu C., Tan K.H., Fung T.C., "Investigations of nonlinear dynamic performance of top-and-seat with web angle connections subjected to sudden column removal", *Engineering Structures*, 99, 449-461, 2015a.

[8] Tyas A., Warren J.A., Stoddart E.P., Davison J.B., Tait S.J., Huang Y., "A methodology for combined rotation-extension testing of simple steel beam to column joints at high rates of loading", *Experimental Mechanics*, 52, 1097-1109, 2012.

[9] Rahbari R., Tyas A., Buick D.J., Stoddart E.P., "Web shear failure of angle-cleat connections loaded at high rates", *Journal of Constructional Steel Research*, 103, 37-48, 2014.

[10] Karns J.E., Houghton D.L., Hong J.-K., Kim J., "Behavior of varied steel frame connection types subjected to air blast, debris impact, and/or post-blast progressive collapse load conditions", Structures Congress 2009, 1-10, 2009.

[11] Grimsmo E.L., Clausen A.H., Langseth M., Aalberg A., "An experimental study of static and dynamic behaviour of bolted end-plate joints of steel", *International Journal of Impact Engineering*, 85, 132-145, 2015.

[12] Grimsmo E.L., Clausen A.H., Aalberg A., Langseth M., "A numerical study of beam-to-column joints subjected to impact", *Engineering Structures*, 120, 103-115, 2016.

[13] *Eurocode 3: Design of steel structures—part 1-1: General rules and rules for buildings.* BS EN 1993-1-1, London, U.K., British Standards Institution, 2005.

[14] *Specification for structural steel buildings.* ANSI/AISC 360-10, Chicago, I.L., U.S., American Institute of Steel Construction, 2010.

[15] *Ls-dyna keyword user's manual*, Livermore Software Technology Corporation, 2007.

[16] Abramowicz W., Jones N., "Dynamic axial crushing of square tubes", *International Journal of Impact Engineering*, 2, 179-208, 1984.